

Quantum phase transition in a dimerized chain with hexamer distortion

Mahboobeh Shahri Naseri^{1,3}, George I. Japaridze², Saeed Mahdavifar^{*1}, and Saber Farjami Shayesteh¹

¹ Department of Physics, University of Guilan, 41335-1914, Rasht, Iran

² College of Engineering, Ilia State University, Cholokashvili Ave. 3-5, 0162 Tbilisi, Georgia

³ Department of Physics, Payame Noor University, 19395-3697, Tehran, Iran

Key words: Dimerized chain, hexamer, spin-1/2

* Corresponding author: e-mail mahdavifar@guilan.ac.ir

We consider the dimerized spin- $\frac{1}{2}$ Heisenberg chain with spin hexameric distortion of the exchange pattern and study the zero-temperature phase diagram in the parameter space (J_1, J_2, J_3) by continuum-limit bosonization approach and the exact diagonalization method. The phase diagram is rich and has two gapped dimer phases.

We obtain an estimate of the critical line separating the different gapped dimer phases by the bosonization approach. The existence of the transition line and the difference between dimer phases is checked numerically. The behavior of the energy gap and the dimer order parameter supports the exact location of the gapless line.

Copyright line will be provided by the publisher

1 Introduction The critical gapless phases emerging on the border lines separating two gapped phases in low-dimensional spin systems has been the subject of studies for decades. The spin $S = 1/2$ Heisenberg chain with dimerization and frustration, is a primer and well studied example of a such system which shows a gapless phase in the ground state phase diagram [1,2,3,4]. After the seminal paper by Martin-Delgado et.al [5], great attention has been focused on the studies of the same phenomena in the other wide class of low-dimensional magnets such as the spin ladders. [6,7,8,9,10,11,12,13,14] Recently, the gapless phases on the border of different massive phases has been discussed in two-dimensional spin systems [15,16,17].

In this paper, we address this problem within the slightly different framework, namely we study the stability of the explicitly dimerized (gapped) Heisenberg chain towards the perturbation caused by the different commensurate modulation of the exchange pattern which higher period itself causes a gapped state however breaks the favored by the explicit dimer order.

The Hamiltonian of the model that under consideration is defined as

$$\hat{H} = \hat{H}_0 + \hat{H}_\lambda, \quad (1)$$

where

$$\hat{H}_0 = J \sum_{n=1}^N (1 - (-1)^n \delta) \mathbf{S}_n \cdot \mathbf{S}_{n+1}, \quad (2)$$

is the Hamiltonian of the dimerized chain with strong odd links ($\delta > 0$) and

$$\hat{H}_\lambda = \lambda J \sum_{n=1}^N g(n) \mathbf{S}_n \cdot \mathbf{S}_{n+1}, \quad (3)$$

where

$$g(n) = 1 + \cos \pi n + 2 \left[\cos\left(\frac{\pi}{3}n\right) + \cos\left(\frac{2\pi}{3}n\right) \right], \quad (4)$$

is the perturbation Hamiltonian of the dimerized chain with commensurate and modulation of the exchange on each 6-th link which increase (decrease) at $\lambda > 0$ ($\lambda < 0$). Here \mathbf{S}_n is the spin $S = \frac{1}{2}$ operator at site n and the chain consists of $N = 6N_0$ sites. It is straightforward to obtain the Hamiltonian Eq. (1), describes a Heisenberg chain with the following hexamer modulation of the spin exchange (see Fig. 1).

$$\begin{aligned} J(1) &= J(3) = J(5) = J(1 + \delta) = J_1 \\ J(2) &= J(4) = J(1 - \delta) = J_2, \\ J(6) &= J(1 - \delta + 6\lambda) = J_3. \end{aligned} \quad (5)$$

Copyright line will be provided by the publisher

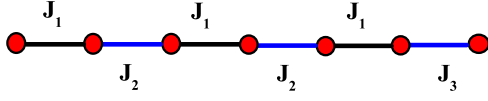


Figure 1 (Color online.) Schematic representation of spin chains with hexameric modulation of spin exchange which is considered in the paper.

In our recent paper [18], we have studied the magnetic phase diagram of the model in the limit of strong exchange on odd links. It has been shown, that the presence of additional modulation leads to the dynamical generation of two new energy scales in the system and to the appearance of two additional quantum phase transitions in the ground state of the system. These new gaps appear at finite magnetization and show themselves in the presence of two new magnetization plateaus at magnetization equal to $\frac{1}{3}$ and $\frac{2}{3}$ of the saturation value.

In this paper, we study the effects caused by the additional distortion of the exchange pattern with period six on the ground state properties of the dimerized chain at zero magnetization. We show that in the case of frustrating character of hexamer distortion, with increasing λ a quantum phase transition takes place in the ground state of the system. The transition corresponds to the reestablishment of the gapless critical phase on the border line, which separates two dimerized phases with shifted in respect to each other on one lattice unit dimer order.

The paper is organized as follows: In the next section, the bosonization method is applied and the transition line is determined analytically. In the section 3, the results of a numerical experiment are presented. Finally, we will discuss and summarize our results in section 4.

2 Bosonization In this Section, we use the continuum-limit bosonization treatment to study the ground state phase diagram of the model (1). To obtain the continuum version of the Hamiltonian, we use the standard bosonization expression of the spin operators [19]

$$S_n^z = \frac{1}{\sqrt{2\pi}} \partial_x \phi(x) + \frac{(-1)^n}{\pi a_0} \sin(\sqrt{2\pi}\phi), \quad (6)$$

$$S_n^x = \cos(\sqrt{2\pi}\theta) \left[1 + \frac{(-1)^n}{\pi a_0} \sin(\sqrt{2\pi}\phi) \right], \quad (7)$$

$$S_n^y = \sin(\sqrt{2\pi}\theta) \left[1 - \frac{(-1)^n}{\pi a_0} \sin(\sqrt{2\pi}\phi) \right]. \quad (8)$$

Here $\phi(x)$ and $\theta(x)$ are dual bosonic fields, $\partial_t \phi = v_s \partial_x \theta$, and satisfy the following commutation relations

$$\begin{aligned} [\phi(x), \theta(y)] &= i\Theta(y-x), \\ [\phi(x), \theta(x)] &= i/2, \end{aligned} \quad (9)$$

and a_0 is the constant of the order of lattice unit. Using (6)-(8), one gets the following bosonized expression for the alternating part of the "dimerization operator"

$$\mathbf{S}_n \cdot \mathbf{S}_{n+1} \sim \frac{(-1)^n}{\pi^2 a_0} \cos(\sqrt{2\pi}\phi(x)), \quad (10)$$

and finally (see for details Ref. [18]) the following continuum-limit bosonized version of the Hamiltonian (1)

$$\begin{aligned} H_{Bos} &= \int dx \left\{ \frac{u}{2} [(\partial_x \phi)^2 + (\partial_x \theta)^2] \right. \\ &\quad \left. - \frac{\Delta_0}{2\pi a_0} \cos(\sqrt{2\pi}\phi) \right\}, \end{aligned} \quad (11)$$

where

$$\Delta_0 = J(\delta - \lambda) = \frac{1}{6}(3J_1 - 2J_2 - J_3), \quad (12)$$

and the velocity of spin excitations

$$u = a_0 J(1 + 6\lambda) \equiv a_0 J_{eff}.$$

From the exact solution of the sine-Gordon model, it is known that for arbitrary finite Δ_0 the excitation spectrum of the Hamiltonian Eq. (11) is gapped and consists of solitons and antisolitons with mass M and soliton-antisoliton bound states ("breathers") with the lowest breather mass also equal to M [20,21]. The soliton mass M , which determines the gap in the excitation spectrum and is connected with bare model parameters (Δ_0 and J_{eff}) as follows $M = J_{eff} \mathcal{C}(\Delta_0/J_{eff})^{2/3}$ where $\mathcal{C} \simeq 1.4$ [22].

The gapped character of the excitation spectrum results to suppression fluctuations in the system and the ϕ field is condensed in one of its vacua ensuring the minimum of the dominating potential energy

$$\langle \phi \rangle = \begin{cases} \sqrt{\pi/2} & \text{at } \Delta_0 < 0 \\ 0 & \text{at } \Delta_0 > 0 \end{cases}. \quad (13)$$

The vacuum expectation value of the *cosine* field in the gapped phase in the weak coupling is given by

$$\epsilon = \langle \cos \sqrt{2\pi}\phi \rangle \simeq (M/J_{eff})^{1/2}, \quad (14)$$

while in the strong coupling, at $|M| \geq J$ it becomes of the unit order [23].

In absence of the hexamer distortion, at $\lambda = 0$ (i.e. $J_2 = J_3 = J(1 - \delta)$), $\Delta_0 = \delta J > 0$, the excitation spectrum is gapped and the field $\phi(x)$ is pinned with vacuum expectation value $\langle \phi \rangle = 0$. Using the bosonized expressions for spin operators one can easily get the on-site spin order is strongly suppressed, while the link-located dimer order

$$\langle \mathbf{S}_n \cdot \mathbf{S}_{n+1} \rangle = Const + (-1)^n \frac{\epsilon}{\pi^2} \quad (15)$$

shows the long-range ordered for dimer order and the maxima of the dimerization functions located on even links.

At $\delta = 0$, i.e. $J_1 = J_2 = J$, $J_3 = J(1 + 6\lambda)$ again the excitation spectrum is gapped, but in this case with the bare mass $\Delta_0 = -\lambda J < 0$. In this case for $\lambda < 0$, $\phi(x)$ is pinned with vacuum expectation value $\langle \phi \rangle = 0$ and for $\lambda > 0$, $\phi(x)$ is pinned with vacuum expectation value $\langle \phi \rangle = \pi$. As a result, fluctuations of the on-site degrees of freedom are fully suppressed, while the link-located dimerization function shows a long range order

$$\langle \mathbf{S}_n \cdot \mathbf{S}_{n+1} \rangle = Const + (-1)^n \text{sign}(\lambda) \frac{\epsilon}{\pi^2}. \quad (16)$$

At $\lambda < 0$, exchange on each 6-th weak link becomes weaker, the dimer order introduced by the hexamer distortion of the spin exchange is once again given by Eq. (15) and therefore as in the case with $\delta > 0$ maxima of the dimerization functions are located on even links.

At $\lambda > 0$ the dimer order is pinned with the strongest links and the minimum of the energy is realized with dimer order which shows maxima on even, including the strongest each 6-th link. Therefore, in marked contrast with $\lambda < 0$ case, at $\lambda > 0$ the hexamer distortion plays the role of frustration with respect to initial explicit dimer order.

Therefore, at finite $\delta > 0$ and $\lambda > 0$, in the gapped phase, the long range ordered dimerization pattern has maxima on odd links at $\Delta_0 > 0$ and on even links, at $\Delta_0 < 0$. In the former case, the distribution of dimers coincides with the order of non-disturbed dimerized chain, while in the case of $\delta_0 = 0$, the order determined with dominant strong links. These two gapped phases with shifted on one lattice unit with respect to each-other pattern of dimers are separated by the critical line where $\Delta_0 = 0$ i.e.

$$3J_1 - 2J_2 - J_3 = 6J(\delta - \lambda) = 0, \quad (17)$$

and the gapless critical phase which described by the gaussian free field is realized.

In order to investigate the detailed behavior of the ground state phase diagram and to test the validity of the picture obtained from continuum-limit bosonization treatment, below in this paper we present results of numerical calculations using the exact diagonalization for finite chains.

3 Numerical experiment In this section, we study the ground state phase diagram of the dimerized Heisenberg chain with spin hexameric distortion of exchange by performing a numerical experiment. One of the remarkable ways in field of numerical experiments is known as the exact diagonalization (ED) method. We have used the ED method to diagonalize numerically the Hamiltonian (1) with periodic boundary conditions. To determine the ground state phase diagram of the model, we have calculated the spin gap and the dimer order parameter as a function of coupling exchange on odd links, J_1 , for finite chains with lengths up to $N = 24$ and different values of exchanges J_2, J_3 .

In Fig. 2, we have presented results of our numerical calculations on the energy gap for the values of

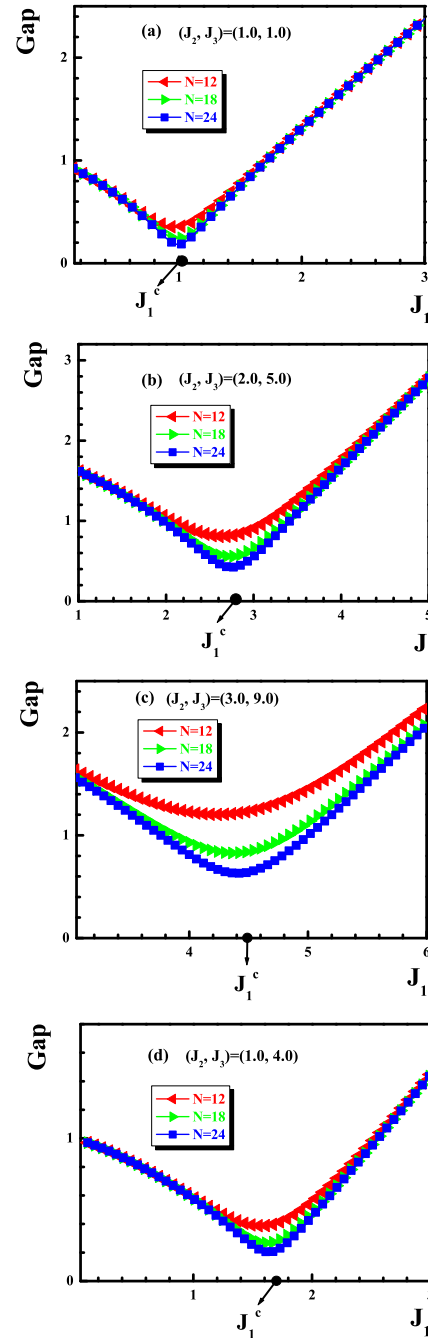


Figure 2 (Color online) The energy gap versus J_1 for the dimerized chains with lengths $N = 12, 18, 24$ and different values of the exchanges $(J_2, J_3) = (a) : (1.0, 1.0)$, $(b) : (2.0, 5.0)$, $(c) : (3.0, 9.0)$ and $(d) : (1.0, 4.0)$.

the exchanges parameter corresponding to $(J_2, J_3) = (a) : (1.0, 1.0)$, $(b) : (2.0, 5.0)$, $(c) : (3.0, 9.0)$ and $(d) : (1.0, 4.0)$ for different chain lengths $N = 12, 18, 24$. We have recognized the energy gap in finite chains as the

difference between the energies of the ground and first excited states. It is clearly seen that the spectrum of the model is gapped at $J_1 = 0$. As soon as the J_1 increases from zero, the energy gap decreases and vanishes at the critical value J_1^c . It is obvious that for finite systems, the energy gap is always finite and only vanishes at certain value J_1^c in the thermodynamic limit $N \rightarrow \infty$. By further increasing of J_1 , the energy gap reopens and behaves almost linearly in respect J_1 . Therefore, the peculiar behavior of the energy gap shows that the system can be found in two different gapped phases by tuning the exchange values.

At $J_1 = 0$, the system reduced into $N/2$ pair of spins in the singlet state. It is completely natural to expect for finding the ground state of the system in a phase with dimerization on even links, so called Dimer-I. On the other hand, in the limit of very strong exchange on odd links, $J_2 = J_3 = 0$, the ground state has the structure of singlets on odd links, so called Dimer-II. So, the competition between two terms in the Hamiltonian should lead to a quantum phase transition between these two dimer phases. It is known that due to the nature of a dimer phase, translation invariance symmetry is broken by one unit cell of the lattice [11]. The structure of the dimer phase can be obtained by studying the dimer order parameter defined as

$$D = \frac{2}{N} \sum_{n=1}^{N/2} \langle Gs | \mathbf{S}_{2n-1} \cdot \mathbf{S}_{2n} - \mathbf{S}_{2n} \cdot \mathbf{S}_{2n+1} | Gs \rangle, \quad (18)$$

where the notation $\langle Gs | \dots | Gs \rangle$ represents the ground state expectation value. It is expected that the dimer order parameter, D , takes the values $\frac{3}{4}$ and $-\frac{3}{4}$ in the saturated Dimer-I and Dimer-II phases respectively. We have presented our numerical results on the dimer order parameter in Fig. 3 for finite chains with lengths $N = 12, 18, 24$ and exchange values $(J_2, J_3) = (a) : (1.0, 1.0), (b) : (2.0, 5.0), (c) : (3.0, 9.0)$ and $(d) : (1.0, 4.0)$. As is clearly seen, in the absence of J_1 , the dimer order parameter is positive and the ground state of the system is in the saturated Dimer-I phase. As soon as the J_1 is added and increased from zero, induced quantum fluctuations reduce the dimer order parameter D and it reaches to zero value at the critical point J_1^c . We found that, taking zero of D at the critical value J_1^c is size-independent which shows its validity in the thermodynamic limit $N \rightarrow \infty$. By more increasing J_1 , the dimer order parameter becomes negative which is the indication of the long-range dimer ordering on odd links, namely Dimer-II phase. In this region, the negative value of D enhances by increasing the exchange J_1 and it tends to the saturation value of the Dimer-II phase.

To find a better physical picture of the gapped dimer phases, we have a look into the microscopic behavior of the system by using our numerical experiment. Since in a unit cell of a hexamer chain (Fig. 1), there are three different links we have calculated the dimerization on each link

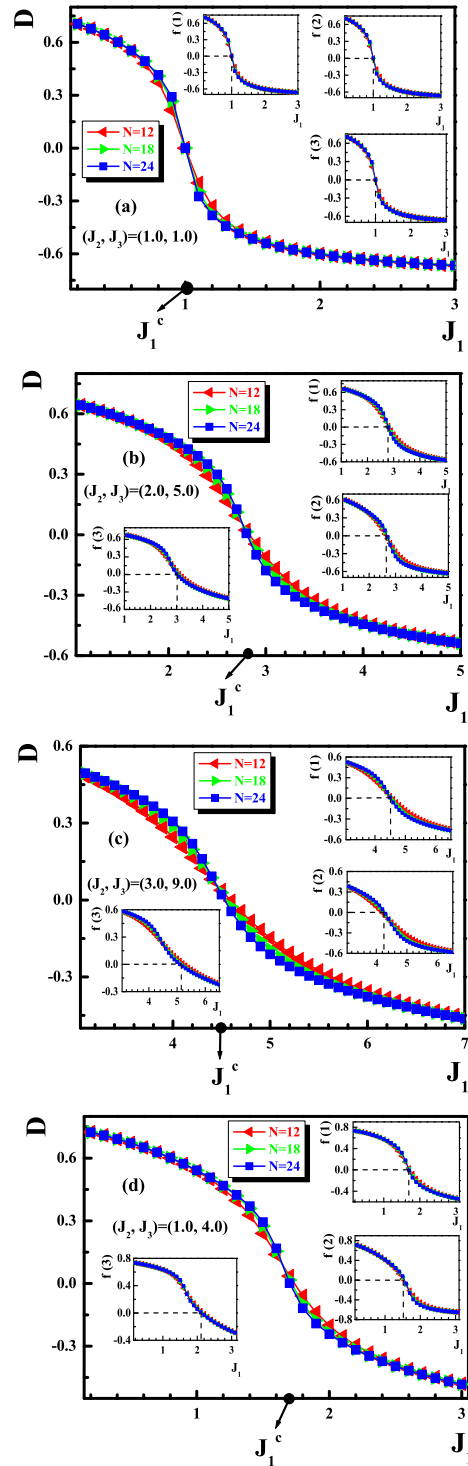


Figure 3 (Color online) The dimer order parameter versus J_1 for the dimerized chains with lengths $N = 12, 18, 24$ and different values of the exchanges $(J_2, J_3) = (a) : (1.0, 1.0), (b) : (2.0, 5.0), (c) : (3.0, 9.0)$ and $(d) : (1.0, 4.0)$. In the inset, the functions $f(1), f(2)$ and $f(3)$ are plotted. The dashed line is only a guide for the eye.

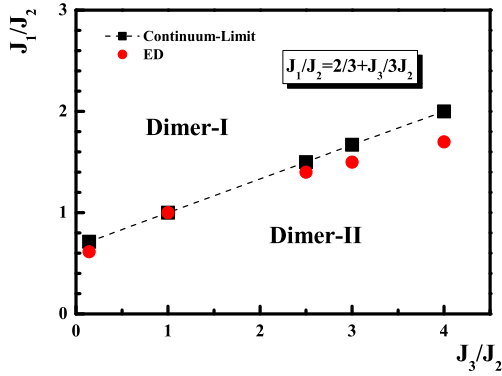


Figure 4 (Color online) The phase diagram of the dimerized Heisenberg chain with hexameric distortion of the exchange pattern. Solid squares are the continuum-limit bosonization data, where solid circles represents the exact diagonalization results extrapolated into the infinite chain limit.

defined as

$$\begin{aligned}
 f(1) &= \langle \mathbf{S}_{6n-5} \cdot \mathbf{S}_{6n-4} - \mathbf{S}_{6n-4} \cdot \mathbf{S}_{6n-3} \rangle, \\
 f(2) &= \langle \mathbf{S}_{6n-3} \cdot \mathbf{S}_{6n-2} - \mathbf{S}_{6n-2} \cdot \mathbf{S}_{6n-1} \rangle, \\
 f(3) &= \langle \mathbf{S}_{6n-1} \cdot \mathbf{S}_{6n} - \mathbf{S}_{6n} \cdot \mathbf{S}_{6n+1} \rangle.
 \end{aligned}
 \tag{19}$$

In the *Inset* of Fig. 3, We have plotted numerical results on these microscopic functions versus the exchange J_1 for chains with lengths $N = 12, 18, 24$ and exchanges $(J_2, J_3) = (a) : (1.0, 1.0), (b) : (2.0, 5.0), (c) : (3.0, 9.0)$ and $(d) : (1.0, 4.0)$. It is clearly seen that the values of functions $f(1), f(2)$ and $f(3)$ take zero at different values of J_1 (dashed lines). By considering the strength of exchanges, expected that the first the dimer on the weakest links takes zero and finally, the strongest one becomes zero which behavior is completely seen in our numerical results.

We have to mention that for other values of the exchanges, we did our numerical experiment as well and found the same ground state magnetic phase diagram contains of: (I.) gapped Dimer-I phase in the region $J_1 < J_1^c$ (II.) gapped Dimer-II phase in the region $J_1 > J_1^c$ (Fig. 4). In this figure, solid squares are the critical points obtained using the continuum-limit bosonization and solid circles represents critical points obtained by numerical experiment. The comparison of numerical results with predictions from the continuum-limit field theory shows well agreement. Besides the above calculations, to obtain the type of the mentioned quantum phase transition between dimer phases in our model, we have implemented the algorithm to find the ground state energy. A very important indication of the first order phase transition is the discontinuity in the first derivation of the ground state energy at

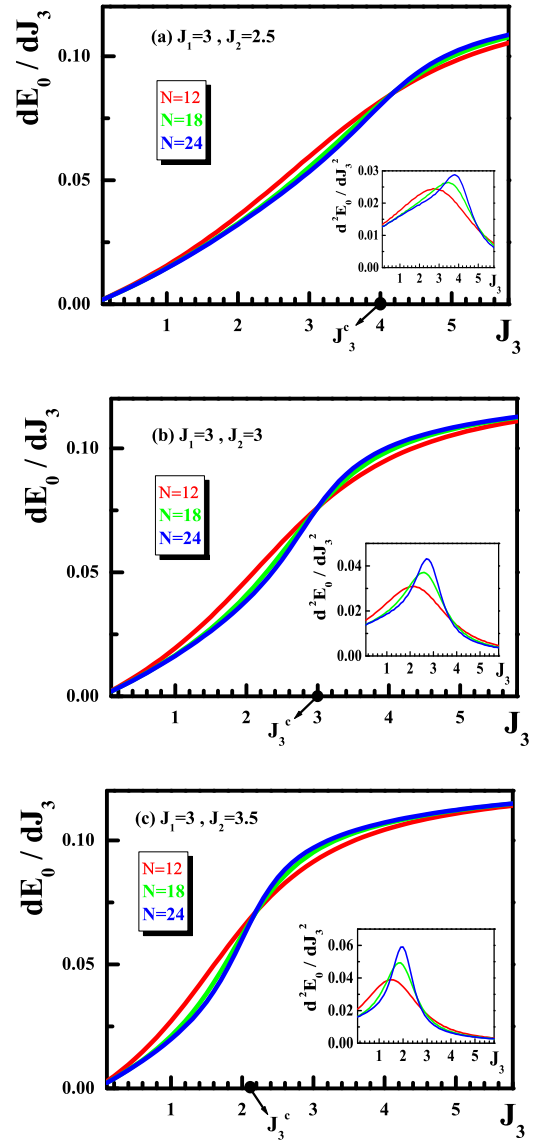


Figure 5 (Color online) The first derivation of the ground state energy as a function of the control parameter J_3 for the dimerized chains with lengths $N = 12, 18, 24$ and different values of the exchanges $(J_1, J_2) = (a) : (3.0, 2.5), (b) : (3.0, 3.0)$ and $(c) : (3.0, 3.5)$. In the inset, the second derivation of the ground state energy are plotted.

the quantum critical point. Using the numerical Lanczos method, we have calculated the ground state energy for chain sizes $N = 12, 18, 24$ and plotted the first derivation of the ground state energy as a function of the control parameter J_3 in the Fig. 5. The results of the first derivation show absence of any discontinuity and therefore in agreement with bosonization studies indicates on the continuous character of the phase transition. Also, we have calculated the second derivation of ground state energy in the inset of Fig. 5. It is clearly seen that the height of peak enhances by increasing J_3 and the second derivation of ground state energy will be diverged in the thermodynamic limit $N \rightarrow \infty$ that is in agreement with the continuous phase transition. The shift in the position of peaks is result of the finite size effect.

4 Conclusions In this paper, we have studied the ground-state properties of the dimerized Heisenberg chain with spin $\frac{1}{2}$, which has hexameric distortion of the exchange pattern. We have determined the existence of a gapless line in the quantum phase diagram by the bosonization technique in the continuum-limit approach. Moreover, the exact diagonalization method has indicated that the ground state has two gaped phases, so called the Dimer-I and Dimer-II phases. Our numerical results are in well agreement with analytical results.

Acknowledgements G. I. Japaridze acknowledges support from the SCOPES Grant IZ73Z0-128058 and the Georgian NSF Grant No. ST09/4-447.

References

- [1] R. Chitra, S. Pati, H. R. Krishnamurthy, D. Sen, and S. Ramasesha, Phys. Rev. B **52**, 6581 (1995).
- [2] G. Bouzerar, A. P. Kampf, and G. I. Japaridze, Phys. Rev. B **58**, 3117 (1998).
- [3] X. F. Jiang, H. Chen, D. Y. Xing, and J. M. Dong, J. Phys.:Condens. Matter **13**, 6519 (2001).
- [4] K. P. Schmidt, C. Knetter, and G. S. Uhrig, Phys. Rev. B **69**, 104417 (2004).
- [5] M. A. Martin-Delgado, R. Shankar, and G. Sierra, Phys. Rev. Lett. **77**, 3443 (1996).
- [6] M. A. Martin-Delgado, J. Dukelsky, and G. Sierra, Phys. Lett. A **250**, 430 (1998).
- [7] V. N. Kotov, J. Oitmaa, and Z. Weihong, Phys. Rev. B **59**, 11377 (1999).
- [8] D. C. Cabra and M. D. Grynberg, Phys. Rev. Lett. **82**, 1768 (1999).
- [9] Y. -J. Wang and A. A. Nersesyan, Nucl. Phys. B **583** [FS], 671 (2000).
- [10] K. Okamoto, Phys. Rev. B **67**, 212408 (2003).
- [11] J. Almeida, M. A. Martin-Delgado, and G. Sierra, Phys. Rev. B **76**, 184428 (2007).
- [12] J. Almeida, M. A. Martin-Delgado, and G. Sierra, Phys. Rev. B **77**, 094415 (2008).
- [13] G. Y. Chitov, B. W. Ramakko, and M. Azzouzn, Phys. Rev. B **77**, 224433 (2008).
- [14] S. J. Gibson, R. Meyer, and G. Y. Chitov, Phys. Rev. B **83**, 104423 (2011).
- [15] V. N. Kotov, D.-X. Yao, A. H. Castro Neto, and D. K. Campbell, Phys. Rev. B **80**, 174403 (2009).
- [16] D. -X. Yao, J. Gustafsson, E. W. Carlson, and A. W. Sandvik, Phys. Rev. B **82**, 172409 (2010).
- [17] L. Fritz, R. L. Doretto, S. Wessel, S. Wenzel, S. Burdin, and M. Vojta, Phys. Rev. B **83**, 174416 (2011).
- [18] M. Shahri Naseri, G. I. Japaridze, S. MahdaviFar, and S. Farjami Shayesteh, J. Phys.:Condens. Matter **24**, 116002 (2012).
- [19] T. Giamarchi, Quantum Physics in One Dimension (Oxford University Press, Oxford, 2004).
- [20] R. F. Dashen, B. Hasslacher, and A. Neveu, Phys. Rev. D **10**, 3424 (1975).
- [21] A. Takhtadjan and L. D. Faddeev, Sov. Theor. Math. Phys. **25**, 147 (1975).
- [22] Al. B. Zamolodchikov, Int. Jour. Mod. Phys. A **10**, 1125 (1995).
- [23] S. Lukyanov and Al. A. Zamolodchikov, Nucl. Phys. B **493**, 571 (1997).

Greek symbols – w-greek.sty

α	<code>\alpha</code>	θ	<code>\theta</code>	o	<code>o</code>	τ	<code>\tau</code>
β	<code>\beta</code>	ϑ	<code>\vartheta</code>	π	<code>\pi</code>	υ	<code>\upsilon</code>
γ	<code>\gamma</code>	ι	<code>\iota</code>	ϖ	<code>\varpi</code>	ϕ	<code>\phi</code>
δ	<code>\delta</code>	κ	<code>\kappa</code>	ρ	<code>\rho</code>	φ	<code>\varphi</code>
ϵ	<code>\epsilon</code>	λ	<code>\lambda</code>	ϱ	<code>\varrho</code>	χ	<code>\chi</code>
ε	<code>\varepsilon</code>	μ	<code>\mu</code>	σ	<code>\sigma</code>	ψ	<code>\psi</code>
ζ	<code>\zeta</code>	ν	<code>\nu</code>	ς	<code>\varsigma</code>	ω	<code>\omega</code>
η	<code>\eta</code>	ξ	<code>\xi</code>				
Γ	<code>\itGamma</code>	Λ	<code>\itLambda</code>	Σ	<code>\itSigma</code>	Ψ	<code>\itPsi</code>
Δ	<code>\itDelta</code>	Ξ	<code>\itXi</code>	Υ	<code>\itUpsilon</code>	Ω	<code>\itOmega</code>
Θ	<code>\itTheta</code>	Π	<code>\itPi</code>	Φ	<code>\itPhi</code>		

Table 1: Slanted greek letters

α	<code>\upalpha</code>	θ	<code>\uptheta</code>	o	<code>\upo</code>	τ	<code>\uptau</code>
β	<code>\upbeta</code>	ϑ	<code>\upvartheta</code>	π	<code>\uppi</code>	υ	<code>\upupsilon</code>
γ	<code>\upgamma</code>	ι	<code>\upiota</code>	ϖ	<code>\upvarpi</code>	ϕ	<code>\upphi</code>
δ	<code>\updelta</code>	κ	<code>\upkappa</code>	ρ	<code>\uprho</code>	φ	<code>\upvarphi</code>
ϵ	<code>\upepsilon</code>	λ	<code>\uplambda</code>	ϱ	<code>\upvarrho</code>	χ	<code>\upchi</code>
ε	<code>\varepsilon</code>	μ	<code>\upmu</code>	σ	<code>\upsigma</code>	ψ	<code>\uppsi</code>
ζ	<code>\upzeta</code>	ν	<code>\upnu</code>	ς	<code>\upvarsigma</code>	ω	<code>\upomega</code>
η	<code>\upeta</code>	ξ	<code>\upxi</code>				
Γ	<code>\Gamma</code>	Λ	<code>\Lambda</code>	Σ	<code>\Sigma</code>	Ψ	<code>\Psi</code>
Δ	<code>\Delta</code>	Ξ	<code>\Xi</code>	Υ	<code>\Upsilon</code>	Ω	<code>\Omega</code>
Θ	<code>\Theta</code>	Π	<code>\Pi</code>	Φ	<code>\Phi</code>		

Table 2: Upright greek letters

α	<code>\bm{\alpha}</code>	θ	<code>\bm{\theta}</code>	o	<code>\bm{o}</code>	τ	<code>\bm{\tau}</code>
β	<code>\bm{\beta}</code>	ϑ	<code>\bm{\vartheta}</code>	π	<code>\bm{\pi}</code>	υ	<code>\bm{\upsilon}</code>
γ	<code>\bm{\gamma}</code>	ι	<code>\bm{\iota}</code>	ϖ	<code>\bm{\varpi}</code>	ϕ	<code>\bm{\phi}</code>
δ	<code>\bm{\delta}</code>	κ	<code>\bm{\kappa}</code>	ρ	<code>\bm{\rho}</code>	φ	<code>\bm{\varphi}</code>
ϵ	<code>\bm{\epsilon}</code>	λ	<code>\bm{\lambda}</code>	ϱ	<code>\bm{\varrho}</code>	χ	<code>\bm{\chi}</code>
ε	<code>\bm{\varepsilon}</code>	μ	<code>\bm{\mu}</code>	σ	<code>\bm{\sigma}</code>	ψ	<code>\bm{\psi}</code>
ζ	<code>\bm{\zeta}</code>	ν	<code>\bm{\nu}</code>	ς	<code>\bm{\varsigma}</code>	ω	<code>\bm{\omega}</code>
η	<code>\bm{\eta}</code>	ξ	<code>\bm{\xi}</code>				
Γ	<code>\bm{\itGamma}</code>	Λ	<code>\bm{\itLambda}</code>	Σ	<code>\bm{\itSigma}</code>	Ψ	<code>\bm{\itPsi}</code>
Δ	<code>\bm{\itDelta}</code>	Ξ	<code>\bm{\itXi}</code>	Υ	<code>\bm{\itUpsilon}</code>	Ω	<code>\bm{\itOmega}</code>
Θ	<code>\bm{\itTheta}</code>	Π	<code>\bm{\itPi}</code>	Φ	<code>\bm{\itPhi}</code>		

Table 3: Boldface variants of slanted greek letters

α	<code>\pmb{\upalpha}</code>	θ	<code>\pmb{\uptheta}</code>	o	<code>\pmb{\upo}</code>	τ	<code>\pmb{\uptau}</code>
β	<code>\pmb{\upbeta}</code>	ϑ	<code>\pmb{\upvartheta}</code>	π	<code>\pmb{\uppi}</code>	υ	<code>\pmb{\upupsilon}</code>
γ	<code>\pmb{\upgamma}</code>	ι	<code>\pmb{\upiota}</code>	ϖ	<code>\pmb{\upvarpi}</code>	ϕ	<code>\pmb{\upphi}</code>
δ	<code>\pmb{\updelta}</code>	κ	<code>\pmb{\upkappa}</code>	ρ	<code>\pmb{\uprho}</code>	φ	<code>\pmb{\upvarphi}</code>
ϵ	<code>\pmb{\upepsilon}</code>	λ	<code>\pmb{\uplambda}</code>	ϱ	<code>\pmb{\varrho}</code>	χ	<code>\pmb{\upchi}</code>
ε	<code>\pmb{\varepsilon}</code>	μ	<code>\pmb{\upmu}</code>	σ	<code>\pmb{\upsigma}</code>	ψ	<code>\pmb{\uppsi}</code>
ζ	<code>\pmb{\upzeta}</code>	ν	<code>\pmb{\upnu}</code>	ς	<code>\pmb{\upvarsigma}</code>	ω	<code>\pmb{\upomega}</code>
η	<code>\pmb{\upeta}</code>	ξ	<code>\pmb{\upxi}</code>				
Γ	<code>\bm{\Gamma}</code>	Λ	<code>\bm{\Lambda}</code>	Σ	<code>\bm{\Sigma}</code>	Ψ	<code>\bm{\Psi}</code>
Δ	<code>\bm{\Delta}</code>	Ξ	<code>\bm{\Xi}</code>	Υ	<code>\bm{\Upsilon}</code>	Ω	<code>\bm{\Omega}</code>
Θ	<code>\bm{\Theta}</code>	Π	<code>\bm{\Pi}</code>	Φ	<code>\bm{\Phi}</code>		

Table 4: Boldface variants of upright greek letters